Resonant Multiport Converter with High Interconnection Capability and Lower Parameter Deviations

Fabian Groon[1], Thiago Pereira[1,2], Sergej Schikowski[3], Dario Metschies[3], Marco Liserre[1,2]

[1] Kiel University, Germany
[2] Fraunhofer Institute for Silicon Technology, Germany
[3] Reese+Techware Industrieelektronik GmbH, Germany

Corresponding author: Fabian Groon, fagr@tf.uni-kiel.de
Speaker: Fabian Groon, fagr@tf.uni-kiel.de

Abstract

DC/DC converters for high-current applications have an important role in onboard systems in electric vehicles (EVs). The converter has to achieve high power density and high efficiency for minimizing weight, maximizing range operation, and saving space in EVs. Further, the interconnection of multiple energy sources becomes crucial in this system for supporting the load at different operation points. Parameter deviations from the transformer and resonant elements can impact the operation of resonant multiport converters by increasing the uneven power flow among the ports and reducing efficiency. Thus, this paper investigates an isolated multiport topology with a reduced number of reactive elements and a planar multiwinding transformer (MWT) to achieve a low parameter deviation and hence balance the power processing in each port of the converter. The causes and effects of this parameter deviation are discussed and the effectiveness of the DC/DC Converter is validated with a prototype.

1 Introduction

Onboard electric vehicle (EV) systems require high power density and high efficiency. The low voltage on the output side, due to the high currents, demands a well-selected topology and optimization to achieve these prerequisites. The design is particularly difficult for onboard EV systems because the input voltage supplied by a battery varies with the type of the battery and the state of charge [1]. Therefore, a wide voltage range is required to achieve the output voltage and power. Regular topologies like LLC and DAB suffer from high conduction losses on the low voltage side. In addition, bidirectional power flow becomes a tendency in such a system, which requires high efficiency also in reverse power flow mode.

Multiport topologies are one solution to this problem. The interconnection on the input or output sides allows for higher power density and high efficiency. These multiport topologies are particularly interesting for low-voltage applications where conduction losses are the limitations. By connecting the output side in parallel, the current can be cut in half to reduce the conduction losses dramatically. Another application for these multiport topologies is to connect different voltage levels to the in- and output and connected several loads to the converter without extra conversion stage [2], [3].

The recently developed GaN HEMTs and SiC MOSFETs allow operations at higher frequencies without increasing the switching losses significantly [4], [5]. This leads to reduced footprint components, especially magnetic components [6], [7]. A trade-off needs to be made for efficiency and power density during the converter design. In this topology, the multiwinding transformer (MWT) is a key component that needs a particular design.

For an optimal operation of the converter, the optimization and design of the MWT are crucial [8]. Litz-wire transformers are cost-benefit, but they suffer from high copper losses at high frequencies [9], [10]. Planar transformers on the other hand are expensive but can achieve higher current densities [11] and do not suffer from the high copper losses like litz-wire [10], [12]. Without multiport topologies, it would be necessary to connect individual transformers between the ports, but power density will be decreased and parameter deviations are high.

ISBN 978-3-8007-6091-6

 DOI:10.30420/566091157

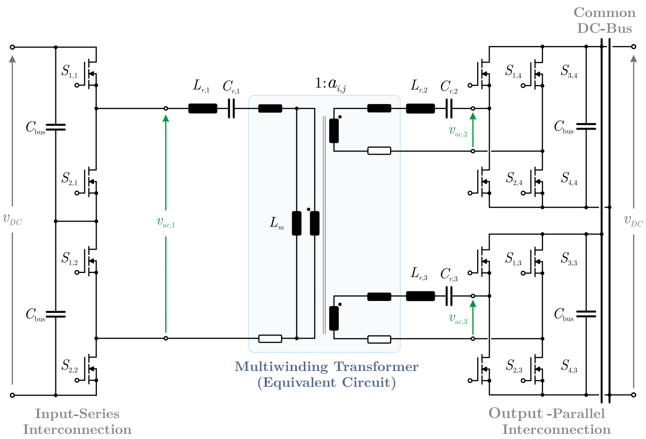

Fig. 1: Proposed resonant converter topology.

These high parameter deviations may arrive from the cores by having different permeability and air gaps due to core assembly or through different turns ratio and leakage inductance. An MWT increases power density and lowers parameter deviation because it does not have the problem of different cores, but still from deviations in turns ratio and leakage inductance.

The interconnection of multiport topologies is difficult, due to parameter deviations [13]. The resonance tanks can also have different parameters and introduce a power-sharing problem in the branches. This not only decreases the efficiency of the converter but also decreases the lifetime of the switches that need to process more power [14]. Therefore, this paper proposes a topology for high-current applications with lower parameter deviations and a wide voltage range. The cause and effects of parameter deviations will be further analyzed. The importance of transformer design is highlighted and a prototype is built to validate the cause of parameter deviations and show the effectiveness of the proposed topology.

The paper is organized as follows: Section II introduces the proposed topology and highlights the advantage over other topologies. Interconnection issues of the multiport converter are explained in Section III. In Section IV a prototype is built and experiments are carried out. Section V concludes this paper.

2 Resonant Multiport Topology with Low Parameter Deviation

The proposed resonant input-series-output-parallel multiport topology is shown in Fig. 1. The input side uses GaN HEMTs and is connected in series to overcome the limited blocking voltage rating of 650 V [15]. The output is connected in parallel and uses Si MOSFETs to minimize conduction losses on the low-voltage side. Si MOSFETs are used instead of GaN HEMTs because the low voltage side is switched with synchronous rectification, where current is measured to turn on and off the switch. Therefore, the switching losses can be almost neglected, since the turn on and off will occur after they already started conducting [16]. The parallel connections reduce the current through each switch by half. Current sharing between the parallel output only depends on the parameters of the resonant tank in both branches and the transformer.

The high-voltage side consists of a half-bridge to lower the component count and increase power density. This is effective since the current is very low and the limitations are the switching losses. The low-voltage side consists of two full bridges to lower the current even further in each switch. The resonant multiport topology allows for bidirectional power flow with high efficiency in both directions. This topology can achieve high efficiencies even in low power conditions. Another advantage of this resonant topology is the wide voltage range. This allows for high efficiencies even if a battery is used as an input over the entire state of charge. Dependent on the application of this converter, the parameters of the resonant tank on the primary and secondary can be designed symmetrical or unsymmetrical to achieve similar or different gain curves in forward and reverse power flow direction [17], [18].

3 Interconnection Issue on Resonant Multiport Converter

DC/DC converters with a low-voltage side generally suffer from high conduction losses, due to high current on the output. These can be reduced by paralleling devices or paralleling bridges, like in the proposed topology in Fig. 1. Paralleling devices have the disadvantage of current sharing problems, because of different $R_{\mathrm{ds(on)}}$ and different threshold voltages, which affect switching losses [19]. When paralleling bridges in a resonant converter, the current sharing is dependent on resonant tank parameter mismatch and transformer. Also Paralleling bridges have a lower stray inductance mismatch than paralleling devices, which results in a lower current imbalance during transient [20].

The deviation can affect the resonance frequency

ISBN 978-3-8007-6091-6

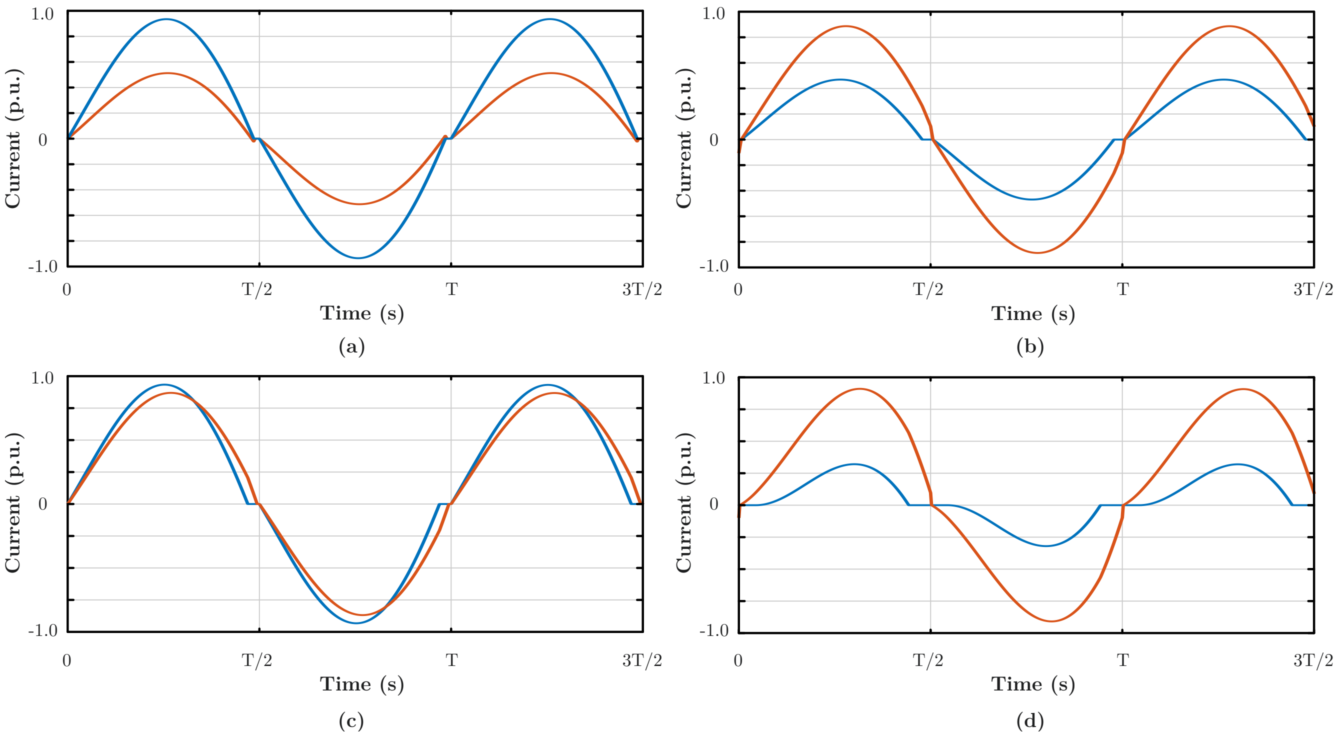

Fig. 2: Simulated mismatch of the proposed converter topology for different cases (a) inductance mismatch (b) turns ratio mismatch (c) inductance compensation for turns ratio mismatch (d) inductance compensation for turns ratio mismatch at different load.

and the current and voltage-sharing ability. Reducing this deviation is crucial to ensure the high efficiency of the converter. The mismatch can arrive from one of the following components and will have a different effect on the waveforms of the current:

– Leakage inductance,
– Transformer turns ratio,
– Capacitor and external inductor.

If the parallel branches have a mismatch in the inductance (leakage or external inductor), then the currents will have the same resonance frequency, but the amplitude is different. This is shown in Fig. 2 (a), where more current flows in one branch than the other. As a result of this, the conduction losses will increase and converter efficiency decreases. The capacitor mismatch has the same influence as the inductance. A mismatch in the transformer turns ratio will result in different resonance frequencies in the branches and different amplitudes, as shown in Fig. 2 (b). This is the worst scenario, since not only the amplitude is different, but the current sharing will change dependent on load and frequency [21], [22].
The amplitude mismatch of the turns ratio can be compensated by an increase of inductance in the branch that has a lower voltage ratio. The higher voltage will be compensated by a higher impedance of inductance, as seen in Fig. 2 (c). The resonance frequency of both branches will still remain different. This compensation will only work in specific working points, where the impedance of the branch is close to the load resistance of the output. When resistance starts to dominate, the compensation will lose its effectiveness as shown in Fig. 2 (d), where a higher output load is connected.
This shows the importance of transformer design for this kind of topology. In conventional litz-wire transformer it is difficult to ensure the exact same turns ratio and the same leakage inductance. Planar transformer on the other hand can be manufactured reliable and will not suffer from this deviation [23]. Another advantage of planar transformer is the controllable leakage and the easy interleaving possibility [24].

4 Experimental Results

The specifications of the built prototype are given in table 1. For the primary side GS-065-060-5-B-A from GaN-Systems and for the secondary side C4D30120D SiC-diodes from Cree are used. The primary side of the setup is shown in Fig. 3 and

 DOI:10.30420/566091157

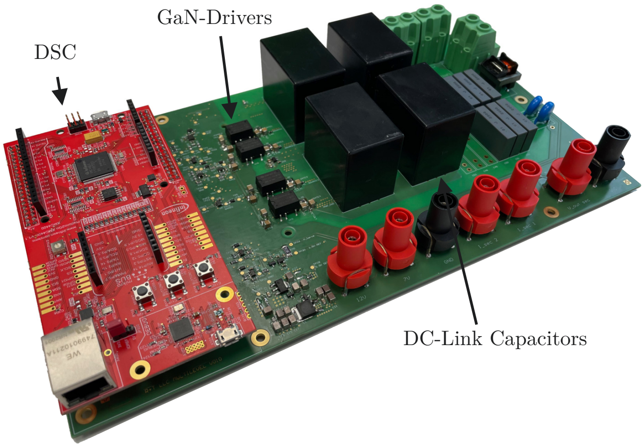

Fig. 3: Primary side of the built prototype.

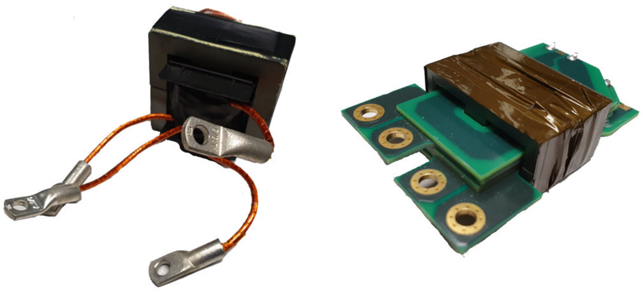

(a) (b)

Fig. 4: Built transformer (a) conventional litz-wire transformer (b) planar transformer.

the conventional litz-wire transformer and planar transformer are shown in Fig. 4 (a) and Fig. 4 (b), respectively. The conventional litz-wire transformer was built with 2 E-cores and litz-wires, where 14 turns for the primary and 2 turns for the secondary were wound around the bobbin of the core. An air-gap was included to achieve the required magnetizing inductance of 92 µH.

The leakage inductance of the transformer was calculated by measuring all open-circuit and short-circuit inductance, and the final leakage was calculated according to [25]. The primary leakage L_{r1} was calculated to be 12.2 µH and the secondary leakage L_{r2} and L_{r3} with 540 nH and 650 nH, respectively. The turns ratio were 7.5:1 and 6.5:1. The low number of turns on the secondary makes it very difficult to achieve equal turns ratio, as already explained in the previous section. Also, the leakage of the transformer is higher than required, because interleaving litz-wires are not as easy as interleaving windings in planar transformers.

In the first measurements shown in Fig. 5 it is clearly visible that there is a high mismatch in the parallel branches and a mismatch in resonance frequency as expected, due to different turns ratio and inductance. One parallel branch is processing double the amount of power and one branch is working in continuous conduction mode and one is in discontinuous conduction mode. This is unfavorable because of high conduction losses and frequency and load-dependent power sharing.

An external inductor was added to the branch that processed more power to compensate for the different turns ratio. The results are shown in Fig. 6, where power-sharing is now improved, but different resonance frequencies still remain. Fig. 6 (a) and (b) shows the waveforms at 650 V and 540 V at 2 kW at above and below resonance frequency, respectively. The waveforms at the same voltage, but lower power at 250 W are given in Fig. 6 (c) and (d), both above the resonance frequency.

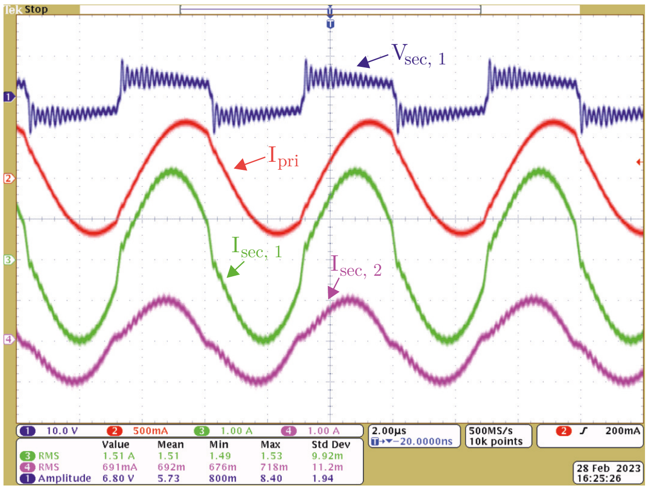

Fig. 5: Measured waveforms with conventional litz-wire transformer and equal external inductors.

Tab. 1: Electrical specifications of the built converter.

Parameter	
Output Power P_{out}	2 kW
Minimum input voltage $V_{\mathrm{in,min}}$	540 V
Maximum input voltage $V_{\mathrm{in,max}}$	760 V
Nominal input voltage $V_{\mathrm{in,nom}}$	650 V
Nominal Output voltage $V_{out,nom}$	48 V
Maximum Output voltage $V_{out,max}$	52 V
Minimum Output voltage $V_{out,min}$	46 V
Nominal switching frequency f_0	200 kHz
Magnetizing inductance L_m	92 μH
Inductance $L_{\mathrm{r1}}, L_{\mathrm{r2}}$	18.6 μH, 380 nH
Capacitance $C_{\mathrm{r1}}, C_{\mathrm{r2}}$	34.2 nF, 1.67 μF
Transformer turns ratio	7:1:1

ISBN 978-3-8007-6091-6

 DOI:10.30420/566091157

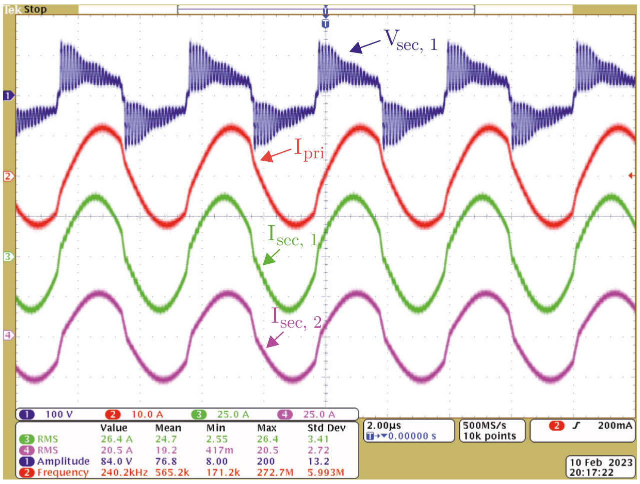

(a)

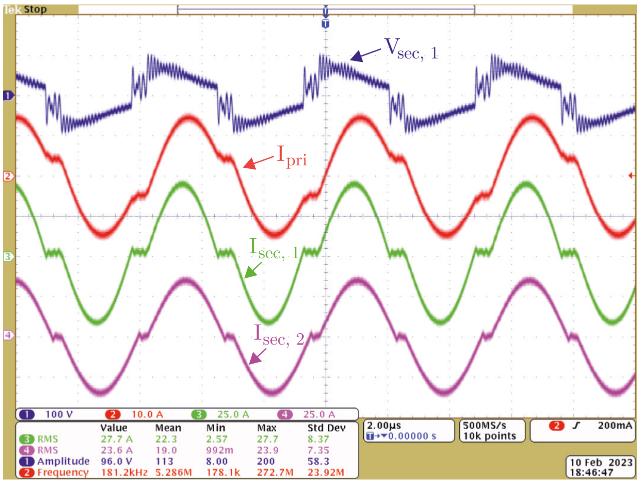

(b)

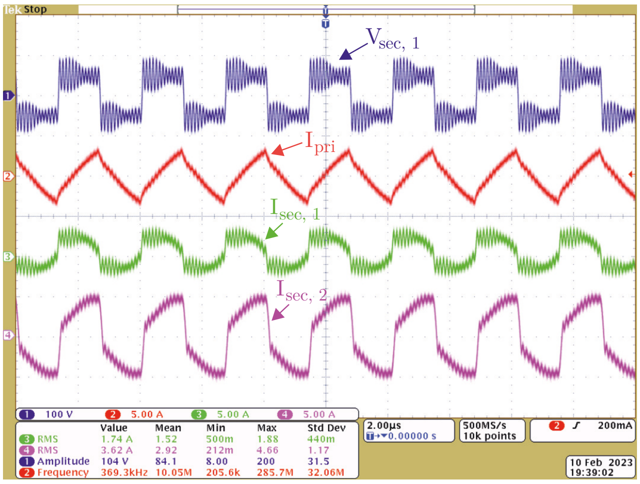

(c)

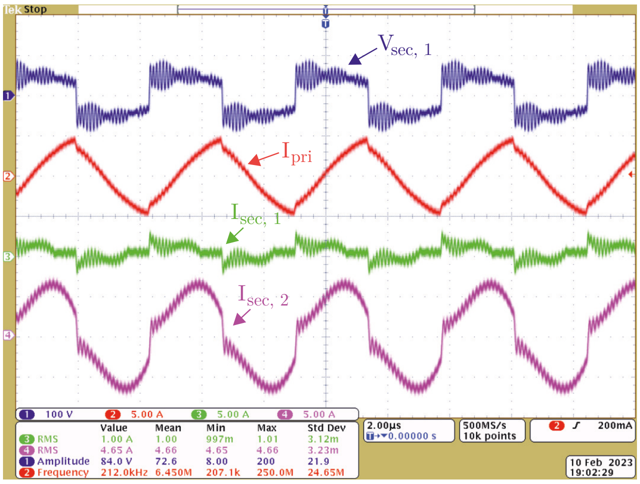

(d)

Fig. 6: Measured waveforms with conventional litz-wire transformer and inductor compensation for (a) 650 V 2 kW, above resonance frequency (b) 540 V 2 kW, below resonance frequency (c) 650 V 250 W, above resonance frequency (d) 540 V 250 W, above resonance frequency.

It is visible that power-sharing is still dependent on frequency and on output resistance. As shown in Fig. 6 the power-sharing is worse at lower frequencies and at higher output resistance. There is an optimal point, where power-sharing is almost equal. To show the advantage of a planar transformer, a prototype was built with 7 turns on the primary and 1 turn each on the secondary. The measured turns ratio was exactly 7:1 for both ports. The leakage inductance was measured as for the litz-wire transformer and the primary leakage L_{r1} was calculated to be 3.5 µH and the secondary leakage L_{r2} and L_{r3} with 110 nH and 110 nH, respectively. This shows the advantage of reliable manufacturing and controllable leakage through interleaving, as here the secondary leakage is below the required inductance value.

The waveforms of the prototype with a planar transformer are shown in Fig. 7 (a) - (d). It is clearly visible that there is only a very small difference in power-sharing which comes from the setup itself and not from the transformer. The parallel branches have the same resonance frequency and power-sharing is guaranteed across all frequency and load ranges.
Finally, the efficiency of the setup was measured. The efficiency is depicted in Fig. 8 and is compared to the theoretically derived efficiency. The measured efficiency is very close to the theoretical efficiency and the maximum efficiency points are also close together. The small deviation in efficiency comes from underestimating diode losses, transformer losses, and final temperatures. A peak efficiency of 92.7 % is achieved at 600 W and an ef-

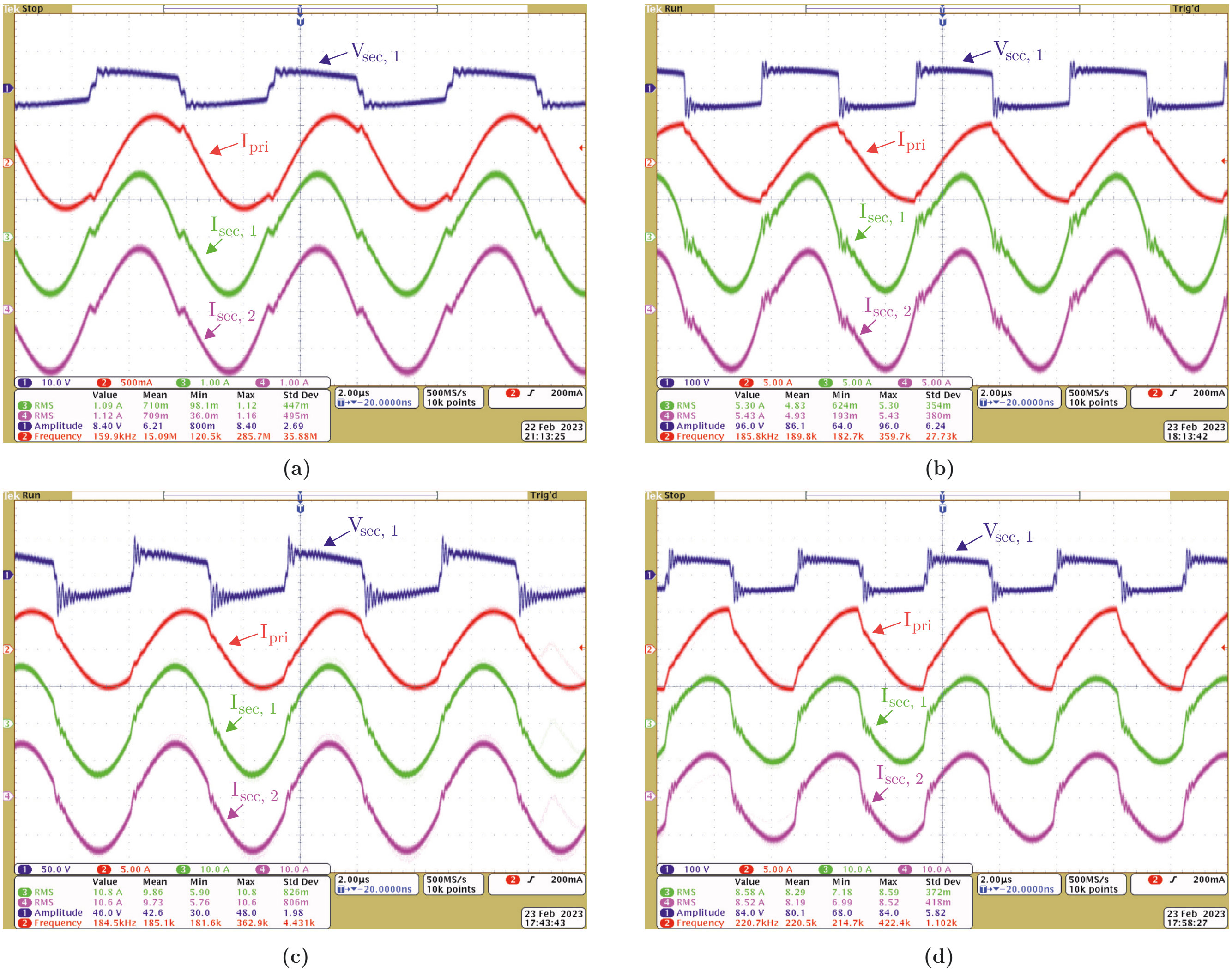

Fig. 7: Measured waveforms at different operation points with a multiwinding planar transformer (a) low power, below resonance frequency (b) medium power, slightly above resonance frequency (c) high power, slightly above resonance frequency (d) high power, above resonance frequency.

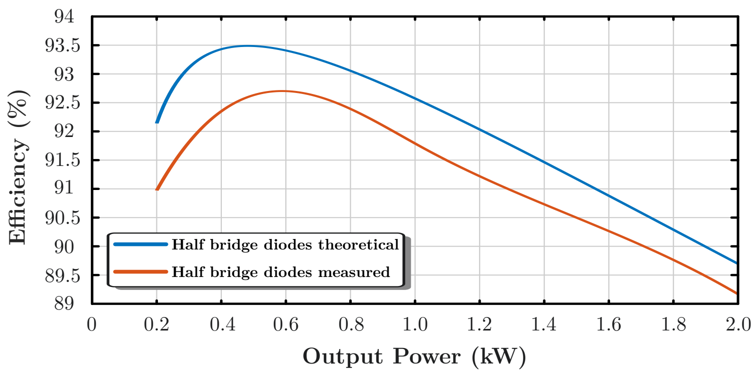

Fig. 8: Measured efficiency and calculated efficiency of the proposed converter with diodes.

ficiency of 89.2 % is achieved at a maximum power rating of 2 kW. If synchronous rectification is used, the efficiency could be increased significantly in the range of above > 97 %, since conduction losses are almost 10 % of the entire losses at full power.

5 Conclusion

This paper presents a topology with lower parameter deviations for high power density and efficiency in high-current applications. The topology is described and advantages and disadvantages are

highlighted. GaN HEMTs are used to achieve the required power density and efficiency.
The interconnection issue is explained and the causes and problems of parameter deviation are shown. Turns ratio and leakage inductance needs to be as equal as possible to achieve power-sharing across all load and frequency ranges. Compensation for turns ratio mismatch can be done to reduce current sharing problems.
A prototype is built to validate the proposed topology. A litz-wire transformer is used to show the effect of parameter deviation and the disadvantage of this type of transformer.
A planar transformer is used to lower parameter deviation to almost zero. The advantage of a planar transformer in this kind of topology is highlighted and the efficiency of the built converter is compared to theoretical calculation. A peak efficiency of 92.7 % with diodes is achieved.

Acknowledgment

We acknowledge the Zentrale Innovationsprogramm Mittelstand (ZIM), which is a funding program of the Federal Ministry for Economic Affairs and Climate Action in Germany for providing financial support (Förderkennzeichen: KK5302202PR1). This research was also funded by the Ministry of Education, Science, and Culture of the state of Schleswig-Holstein, Germany.

References

[1] F. Krismer and J. W. Kolar, “Accurate power loss model derivation of a high-current dual active bridge converter for an automotive application,” IEEE Trans. Ind. Electron., vol. 57, no. 3, pp. 881–891, Mar. 2010.

[2] S. Bandyopadhyay, P. Purgat, Z. Qin and P. Bauer, ”A Multiactive Bridge Converter With Inherently Decoupled Power Flows,” in IEEE Transactions on Power Electronics, vol. 36, no. 2, pp. 2231-2245, Feb. 2021, doi: 10.1109/TPEL.2020.3006266.

[3] J. Schäfer, D. Bortis and J. W. Kolar, ”Multi-port multi-cell DC/DC converter topology for electric vehicle’s power distribution networks,” 2017 IEEE 18th Workshop on Control and Modeling for Power Electronics (COMPEL), Stanford, CA, USA, 2017, pp. 1-9, doi: 10.1109/COMPEL.2017.8013326.

[4] Y. Wu, M. Jacob-Mitos, M. L. Moore and S. Heikman, ”A 97.8% Efficient GaN HEMT Boost Converter With 300- W Output Power at 1 MHz”, IEEE Electron Device Letters, vol. 29, No. 8, August 2008

[5] Y. -F. Wang, B. Chen, Y. Hou, Z. Meng and Y. Yang, ”Analysis and Design of a 1-MHz Bidirectional Multi-CLLC Resonant DC–DC Converter With GaN Devices,” in IEEE Transactions on Industrial Electronics, vol. 67, no. 2, pp. 1425-1434, Feb. 2020, doi: 10.1109/TIE.2019.2899549.

[6] C. Fei, F. C. Lee and Q. Li, ”High-Efficiency High-Power-Density LLC Converter With an Integrated Planar Matrix Transformer for High-Output Current Applications,” in IEEE Transactions on Industrial Electronics, vol. 64, no. 11, pp. 9072-9082, Nov. 2017, doi: 10.1109/TIE.2017.2674599.

[7] M. Mu and F. C. Lee, ”Design and Optimization of a 380–12 V High-Frequency, High-Current LLC Converter With GaN Devices and Planar Matrix Transformers,” in IEEE Journal of Emerging and Selected Topics in Power Electronics, vol. 4, no. 3, pp. 854-862, Sept. 2016, doi: 10.1109/JESTPE.2016.2586964.

[8] Beiranvand, H., Rokrok, E. and Liserre, M. (2020), Vf-constrained ηρ-pareto optimisation of medium frequency transformers in ISOP-DAB converters. IET Power Electronics, 13: 1984-1994. https://doi.org/10.1049/iet-pel.2019.1159

[9] M. Bartoli, N. Noferi, A. Reatti and M. K. Kazimierczuk, ”Modeling Litz-wire winding losses in high-frequency power inductors,” PESC Record. 27th Annual IEEE Power Electronics Specialists Conference, Baveno, Italy, 1996, pp. 1690-1696 vol.2, doi: 10.1109/PESC.1996.548808.

[10] A. H. Wienhausen, A. Sewergin, S. P. Engel and R. W. De Doncker, ”Highly efficient power inductors for high-frequency wide-bandgap power converters,” 2017 IEEE 12th International Conference on Power Electronics and Drive Systems (PEDS), Honolulu, HI, USA, 2017, pp. 442-447, doi: 10.1109/PEDS.2017.8289111.

[11] F. Groon, H. Beiranvand, T. Pereira, G. Can and M. Liserre, ”PCB Layer Optimization of Planar Medium Frequency Transformer for On-Board EV Chargers,” 2022 24th European Conference on Power Electronics and Applications (EPE’22 ECCE Europe), Hanover, Germany, 2022, pp. P.1-P.9.

[12] M. H. Nguyen and H. Fortin Blanchette, “Optimizing AC Resistance of Solid PCB Winding,” Electronics, vol. 9, no. 5, p. 875, May 2020, doi: 10.3390/electronics9050875.

[13] T. Pereira, F. Hoffmann, R. Zhu and M. Liserre, ”A Comprehensive Assessment of Multiwinding Transformer-Based DC–DC Converters,” in IEEE Transactions on Power Electronics, vol. 36, no. 9, pp. 10020-10036, Sept. 2021, doi: 10.1109/TPEL.2021.3064302.

[14] G. Buticchi, M. Andresen, M. Wutti and M. Liserre, ”Lifetime-Based Power Routing of a Quadruple Active Bridge DC/DC Converter,” in IEEE Transactions on Power Electronics, vol. 32, no. 11, pp. 8892-8903, Nov. 2017, doi: 10.1109/TPEL.2017.2650258.

[15] B. N. Pushpakaran, A. S. Subburaj, and S. B. Bayne, “Commercial GaN-based power electronic systems: A review,” Journal of Electronic Materials, vol. 49, no. 11, pp. 6247–6262, Nov. 2020

[16] Xuefei Xie, Joe Chui Pong Liu, F. N. K. Poon and Man Hay Pong, ”A novel high frequency current-driven synchronous rectifier applicable to most switching topologies,” in IEEE Transactions on Power Electronics, vol. 16, no. 5, pp. 635-648, Sept. 2001, doi: 10.1109/63.949496.

[17] J. Min and M. Ordonez, ”Bidirectional Resonant CLLC Charger for Wide Battery Voltage Range: Asymmetric Parameters Methodology,” in IEEE Transactions on Power Electronics, vol. 36, no. 6, pp. 6662-6673, June 2021, doi: 10.1109/TPEL.2020.3033982.

[18] J. Min and M. Ordonez, ”Asymmetric Parameters Design for Bidirectional Resonant CLLC Battery Charger,” 2020 IEEE Energy Conversion Congress and Exposition (ECCE), Detroit, MI, USA, 2020, pp. 5375-5379, doi: 10.1109/ECCE44975.2020.9236171.

[19] G. Wang, J. Mookken, J. Rice and M. Schupbach, ”Dynamic and static behavior of packaged silicon carbide MOSFETs in paralleled applications,” 2014 IEEE Applied Power Electronics Conference and Exposition - APEC 2014, 2014, pp. 1478-1483

[20] H. Li et al., ”Influence of Paralleling Dies and Paralleling Half-Bridges on Transient Current Distribution in Multichip Power Modules,” in IEEE Transactions on Power Electronics, vol. 33, no. 8, pp. 6483-6487, Aug. 2018

[21] T. Pereira, Y. Pascal, M. Liserre, Y. Wei and H. A. Mantooth, ”Multiport Resonant DC-DC Converter using Actively-Controlled Inductors for Hybrid Energy Storage System Integration,” 2022 IEEE Applied Power Electronics Conference and Exposition (APEC), Houston, TX, USA, 2022, pp. 1154-1161, doi: 10.1109/APEC43599.2022.9773497.

[22] T. Pereira, Y. Wei, Y. Pascal, H. A. Mantooth and M. Liserre, ”Self-Tuning Multiport Resonant DC/DC Converter Based on Actively-Controlled Inductors for Hybrid Storage System Integration,” in IEEE Transactions on Power Electronics, vol. 38, no. 4, pp. 4787-4804, April 2023, doi: 10.1109/TPEL.2022.3232188.

[23] Z. Ouyang and M. A. E. Andersen, ”Overview of Planar Magnetic Technology—Fundamental Properties,” in IEEE Transactions on Power Electronics, vol. 29, no. 9, pp. 4888-4900, Sept. 2014, doi: 10.1109/TPEL.2013.2283263.

[24] A. Chandwani and A. Mallik, ”Parametric Modeling and Characterization of Leakage-Integrated Planar Transformer for CLLC DC–DC Converter,” in IEEE Transactions on Magnetics, vol. 58, no. 6, pp. 1-8, June 2022, Art no. 8600308, doi: 10.1109/TMAG.2022.3164599.

[25] H. Beiranvand, F. Hoffmann, Y. Pascal, F. Hahn and M. Liserre, ”Multiwinding Transformer Leakage Inductance Optimization for Power Flow Decoupling in Multiport DC-DC Converters,” 2021 IEEE 15th International Conference on Compatibility, Power Electronics and Power Engineering (CPE-POWERENG), Florence, Italy, 2021, pp. 1-8, doi: 10.1109/CPE-POWERENG50821.2021.9501085.